4 Thermal-infrared asteroid observations at the IRTF

The Infrared Telescope Facility (IRTF) is a 3.0 m telescope on Mauna Kea / Hawai'i, which is optimized for infrared observations of Solar-System objects. It is operated by the Institute for Astronomy (University of Hawai'i) under a cooperative agreement with NASA. Observing time with the IRTF is made available twice a year in an international open competition.

We have been awarded IRTF time for thermal-infrared observations of asteroids in the semesters 2004A, 2004B, 2005A, and 2005B. Techniques have been established to perform IRTF observations remotely from Berlin. We have used the Mid-InfraRed Spectrometer and Imager (MIRSI) and the optical CCD camera "Apogee," the latter for support observations. This thesis also contains IRTF thermal-infrared data which have been obtained with the JPL Mid-InfraRed Large-well Imager (MIRLIN). MIRLIN was replaced at the IRTF by MIRSI in 2003.

This chapter contains a brief description of the capabilities of IRTF, MIRSI, and Apogee as needed for our purposes, followed by a section about the remote observing technique established by us (sect. 4.2). We then explain our observing strategies (sect. 4.3) and detail the data reduction techniques used by us (sect. 4.4).

4.1 IRTF setup and instrumentation

The IRTF is part of the Mauna Kea Observatory / Hawai'i (IAU observatory code 568). Mauna Kea is among the most favorable locations for infrared telescopes worldwide owing to its altitude of some 4200 m above sea level, low atmospheric humidity, and good seeing.

The IRTF is a Cassegrain telescope optimized for infrared astronomy. Its primary mirror has an aperture of 3.0 m. It can be pointed to declinations between +67° and -56° at an hour angle within ±5 h. Differential tracking can be used
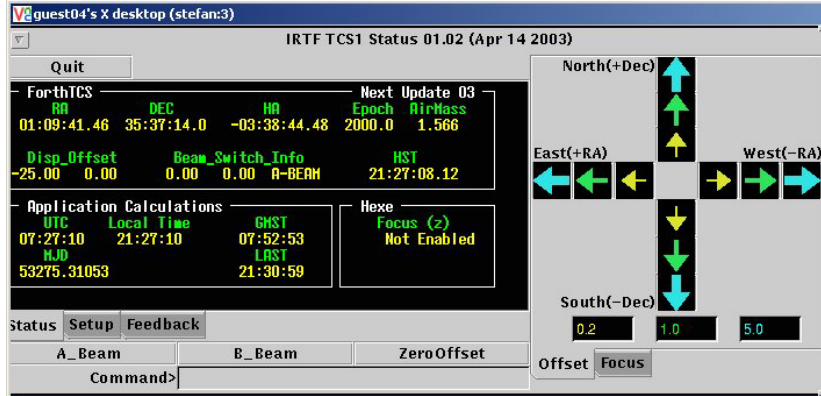
Figure 4.1: tcs1_status, the IRTF tool for focusing and fine tuning of pointing (screenshot from a DLR machine during an IRTF observing run on 27 Sept. 2004).

for for observations of Solar-System objects including NEAs with fast apparent motion.

The Cassegrain secondary mirror provides a $f/35$ beam at the Cassegrain focus where the science instruments are typically situated (an additional Coudé focus is available). IRTF imaging is diffraction limited at mid-infrared wavelengths. The Cassegrain secondary mirror can be oscillated at a frequency up to 40 Hz at a maximum projected amplitude of $6'$, which is important for, e.g., MIRSI observations ("chopping"; see sect. 4.1.1).

Up to four science instruments can be mounted simultaneously at the Cassegrain focus, instrument change-over can normally be accommodated within 30 min; significantly faster in the case of changes between MIRSI and Apogee, which require only a filter to be moved and require only a few seconds.

The telescope shutter consists of two parts for airmass ranges of up to 1.5 (maximum zenith distance $\sim 48°$, only one shutter part open) or up to 2.9 (both parts open) (see eqn. 4.1 on p. 96 for a definition of airmass).

Telescope pointing and tracking is done by the Telescope Operator (TO) who also sets up the instruments. Focusing and fine tuning of the pointing is in the responsibility of the observer; the IRTF software tcs1_status is used for this purpose (see Fig. 4.1).[1]

---

[1] See `http://irtfweb.ifa.hawaii.edu/observing/remote_obs/tcs1_status.pdf`.

Table 4.1: Overview of MIRSI filters used in our programs, together with their estimated 1σ point-source sensitivity in 1 min on-source integration time if mounted on the IRTF (source: Deutsch et al., 2003, for the filter specifications and `http://cfa-www.harvard.edu/mirsi/mirsi_spec.html` for the sensitivities).

Central wavelength (µm)	Width (%)	1σ sensitivity for 1 min integration (mJy)
4.9	21	16.2
7.8	9.0	46.3
8.7	8.9	59.1
9.8	9.4	19.7
11.7	9.9	24.0
12.3	9.6	(no value given)
18.4	8.0	57.3
24.8	7.9	(no value given)

4.1.1 MIRSI

The Mid-Infrared Spectrometer and Imager MIRSI is a mid-infrared camera with imaging capabilities between ~ 5 and 26 µm and additional spectroscopic capabilities over the 8–14 and 17–26 µm atmospheric windows. MIRSI has been built at the Boston University (Deutsch et al., 2003) and has been commissioned at the IRTF in 2003, replacing MIRLIN. It is not an IRTF facility instrument but has been made available by the instrument PI (the late L. Deutsch; now J. Hora) on a collaborative basis. The MIRSI detector is operated at a temperature between 6–12 K inside a helium cooled dewar. The MIRSI control computer system is connected to the IRTF mirror control unit such that it can control chop and nod movements (see below).

Our programs make use of MIRSI in imaging mode, the spectroscopy mode is disregarded in the following. The Si:As impurity-band-conduction detector has 320×240 pixels at a projected pixel scale of $0.27''$ when mounted on the IRTF, corresponding to a field-of-view (FOV) size around $85'' \times 64''$. At MIRSI wavelengths, IRTF imaging is diffraction limited. See table 4.1 for a list of MIRSI filters used in our observations.

Due to the high level of background radiation, single MIRSI exposures (frames) typically saturate within fractions of a second, depending on the filter and on atmospheric conditions. MIRSI observations therefore consist of long series of frames, where the desired frame time and total on-source integration time are set by the observer. Depending on the observing mode, observations are taken at

different positions to enable correction for background radiation. For our observations, MIRSI was used in chop/nod mode. In chop/node mode, MIRSI commands the telescope's Cassegrain secondary mirror to "chop", i.e. to oscillate in a square wave pattern of a user-defined frequency and amplitude (4 Hz and $20''$, in our case). At each chop position, an integer number of frames is taken. Half of the total integration time is chopped at the specified location, then the primary mirror is slewed ("nodded") to an offset position where a second chop set is taken. Combining chopping and nodding enables more accurate subtraction of background radiation (see, e.g., Delbo', 2004, sect. 3.3, for a detailed discussion). The data obtained in a chop/nod exposure are stored as a single FITS file with three extensions where each of the four contained images is the sum of all frames taken at one particular beam position.

The directions and amplitudes of the chop and nod movements are set by the TO upon the observer's request. Timing parameters are specified by the observer through the MIRSI control software.

Due to overheads for, e.g., detector read-out or wait times for the secondary mirror to settle after a chop movement, there is a significant difference between the integration time (i.e. the total time spent collecting measured photons) and the image acquisition time (integration time plus all overheads). All other parameters kept constant, shortening the frame time increases the ratio of acquisition time over integration time.

In the windows opened by the MIRSI control software (see Fig. 4.2, see also `http://www.cfa.harvard.edu/mirsi/MIRSI_Obs_Guide.pdf` for a user guide), the observer specifies the observing mode and corresponding timing parameters, and controls the filter wheel. Information about the target can be entered; this is used by the software to store the target name and the airmass in the header of the resulting FITS file (in addition to the filter used, observation time and duration, etc.). Note that the airmass is *not* taken directly from the telescope control system (such as that displayed in tcs1_status; see Fig. 4.1) but is rather calculated from the system date, the telescope coordinates, and the target RA and dec. entered in the target information form—for the latter, it is important to strictly keep the format described in the observer guide because otherwise the program will crash, typically requiring a lengthy reboot of the control computer and instrument re-initialization.
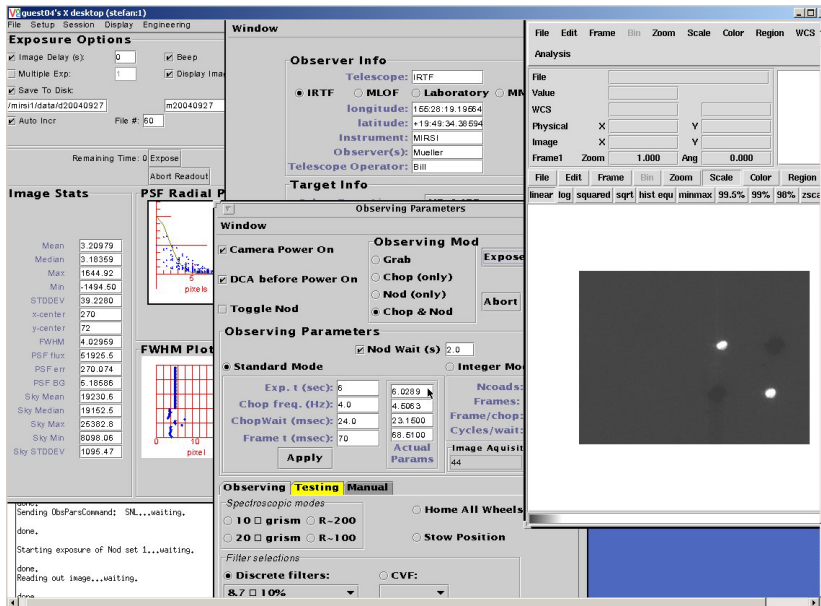
Figure 4.2: Screenshot of the MIRSI control software during a remote IRTF observing run on 27 Sept. 2004.

4.1.2 Apogee

Apogee is an optical-wavelength camera using a commercial 1024×1024 pixel CCD with a field of view of $66''$. Several filters are available, we used a standard V filter in all our observations. Apogee is thermoelectrically cooled to an operational temperature of $-30\,°C$ to reduce the noise level. We typically used Apogee in 4×4–binning mode (thus shrinking the FOV to 256×256 pixels) to reduce the required detector readout times. Changeover between MIRSI and Apogee or vice-versa takes only a few seconds, enabling nearly-simultaneous optical photometry of MIRSI targets to be obtained.

Apogee is significantly more sensitive to asteroid flux than MIRSI. Using the V filter, signal-to-noise ratios exceeding 100 are reached within a few tens of seconds for all asteroid targets which are sufficiently bright for MIRSI observations.

The Apogee control software automatically saves all obtained data in `FITS` format.

4.2 Remote control of observations

The IRTF supports remote control of observations using MIRSI and Apogee. We have established techniques to remotely control IRTF observations from DLR

Berlin and have successfully observed remotely a number of times.[2]

During remote observations, the control programs for both MIRSI and Apogee are executed locally at the IRTF, but the screen output and input from mouse and keyboard can be transferred to/from any computer with access to the internet. For this purpose the VNC protocol is used, which is encrypted and password-protected. A VNC viewer program is required to run on the observer's machine.[3] MIRSI and Apogee require one virtual VNC desktop each. Additionally, observers require access to the program tcs1_status for focusing and pointing fine-tuning.[4] It is advisable to run tcs1_status on another computer within the Institute for Astronomy network. To remotely connect to the machine running tcs1_status from a Windows machine in Berlin, it is most convenient to open a third VNC server on the Hawai'i machine running tcs1_status.

Each VNC server on a machine is identified with its desktop number, which are counted upward starting with 1 (desktop 0 is the native desktop which cannot usually be forwarded). VNC communication between two computers is performed through designated ports, where the default port for a virtual desktop with number n is $5900 + n$. Remote control of IRTF observations thus requires the ports 5901, 5902, and 5903 by default. These ports are blocked by the DLR firewall, and the DLR IT administration is reluctant to open them. Instead, these ports were "tunneled" using an encrypted SSH connection.

In addition to the VNC connections, a channel for direct communication with the telescope operator is required. The IRTF default for remote observers is a PolyCom system or, alternatively, a PC running NetMeeting. Since neither possibility was easily feasible from within the DLR network (and because telephone contact over several hours of observing time would have been rather expensive and inconvenient), we proposed an alternative solution which is now among the default options offered by the IRTF, namely voice-over-IP communication.

The Mauna Kea Weather Center (`http://hokukea.soest.hawaii.edu/index.cgi`) holds many useful resources to remotely check the atmospheric conditions above Mauna Kea. Astronomy-minded weather forecasts for the summit are available (which generally differ vastly from forecasts for the rest of the island) in addition to real-time webcam images from several telescopes at Mauna Kea, real-time meteograms from several telescopes, and nearly-real-time satellite imagery.

---

[2] See also `http://solarsystem.dlr.de/HofW/nr/245/`.

[3] Freeware VNC viewers are available for UNIX/Linux and Windows platforms at `http://www.realvnc.com/`.

[4] See `http://irtfweb.ifa.hawaii.edu/observing/remote_obs/tcs1_status.pdf`.
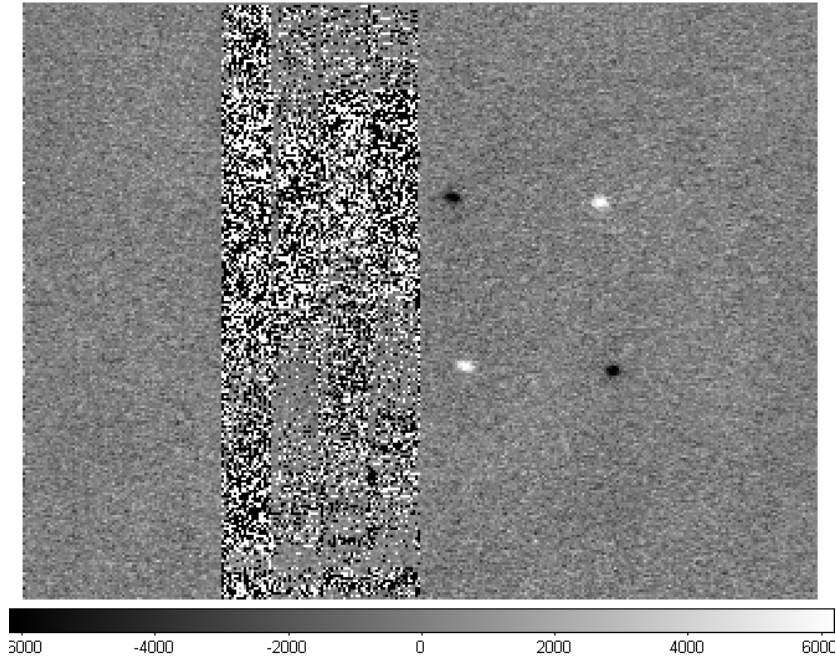
Figure 4.3: Coadded and subtracted MIRSI image with the four beams not quite at the nominal position. Note the artefact pattern in the left half of the detector. (Observation of Itokawa, 10 July 2004, 12:53 UT—this frame could not be used to measure the target flux, see table 6.2 on p. 147)

A particularly useful tool is the CFHT "skyprobe" (`http://www.cfht.hawaii.edu/Instruments/Skyprobe/`) for estimates of the atmospheric extinction. Significant changes in the extinction typically indicate the presence of clouds. After each observing run, we typically save a copy of the skyprobe plot for the respective night, in addition to a Mauna-Kea meteogram, in order to enable later assessment of the atmospheric conditions.

4.3 IRTF observing strategy

General considerations   All MIRSI observations are performed in chop/nod mode to enable subtraction of the celestial background. Since our targets are not spatially resolved, the directions of the chop and nod throws are uncritical; we used $20''$ East-West and North-South, respectively. We used a chop frequency of 4 Hz, a chop wait time of 24 ms, and a nod wait time of 2 s.

No flatfield for MIRSI is available and it would be very time consuming to obtain one; to minimize the possible effect of pixel-to-pixel variations in detector

sensitivity, we have aimed at keeping all sources at a constant position on the chip using tcs1_status. We chose a nominal position such that the center of the four beam positions is centered in the detector's y coordinate and at 75 % in the x direction, where the latter is motivated by the fact that the detector's "left" half is occasionally malfunctioning (see Fig. 4.3 on p. 91). The FOV is large enough to have all four beam positions on the chip, nevertheless.

Apogee observations are interspersed between the MIRSI observations. As for MIRSI, no flatfield is available for Apogee. The telescope is not moved between MIRSI and Apogee observations, such that also for Apogee the on-chip target position is reasonably constant, minimizing the possible effect of pixel-to-pixel variations in sensitivity. Apogee is used with a standard V filter in all our observations.

Calibration observations and observation planning   To facilitate the derivation of absolutely calibrated infrared fluxes and optical V-magnitudes, suitable calibration standard stars are chosen from the lists of Cohen et al. (1996, 1999, for MIRSI) and Landolt (1973, 1992, for Apogee, we picked calibration standards of similar spectral class to the Sun) for each observing run. Calibration standards are typically observed at the beginning and at the end of each observing run. If the atmospheric conditions appear slightly unstable, further calibration observations are interspersed between the target observations to gage the atmospheric stability. To facilitate accurate correction for atmospheric extinction (also called airmass correction, see eqn. 4.2 on p. 96), calibration standards are typically observed at airmasses which bracket those of the primary scientific targets. If the target airmasses span a large range, a calibrator at an intermediate airmass is observed to gage the quality of the airmass correction. Whenever possible, the same calibration standard star is used for all required airmasses (i.e. it is reobserved at a later time) to minimize any possible cross-calibration problems.

The observations are planned such that the science targets are observed at the minimum possible airmass. We furthermore aim at minimizing the number of required changes to the telescope shutter (see sect. 4.1) which occur when the telescope pointing transgresses an airmass boundary value of 1.5.

Starting an observing run   After starting and initializing all required control units for the telescope itself and the instruments, and, in the case of remote observations, after establishing all required communication channels, the instruments

must be initialized (most of these tasks are performed by the TO but may require observer input).

As soon as the instruments are initialized, the telescope should be slewed to a bright MIRSI target, typically a calibration standard star, to focus the telescope using tcs1_status (see Fig. 4.1 on p. 86). Telescope focus is a function of local temperature, therefore it is required to check occasionally during an observation run whether the telescope is still focused, particularly in the first half of the night when the telescope dome cools down significantly.

At the same time, suitable frame times have to be determined for each MIRSI filter to be used during the night: Frame times are limited by the requirement that the sky background, which vastly dominates the flux at MIRSI wavelengths, must not bring the detector close to saturation, so that the detector response to the source flux remains linear. On the other hand, frame times should be as long as possible to optimize the time efficiency of MIRSI observations (see sect. 4.1.1). Background levels can vary greatly on a night-to-night basis, so the optimum frame time must be determined for each MIRSI filter and each observing run. The MIRSI software analyses observational data "on the fly" and displays, among other things, the average, median, and maximum value of sky background radiation (see Fig. 4.2 on p. 89). Frame times should be chosen which bring the average sky level to values not greatly exceeding 20,000 as displayed by the MIRSI control software (Bus, 2004, private communication). Once determined, the filter-dependent frame times should be used throughout the observing run. Significant changes in the sky background during the night typically indicate non-photometric conditions, with the exception that sky levels grow moderately with airmass and furthermore during twilight.

As soon as Apogee has reached its operational temperature of $-30\,°C$, we take a number of bias frames. Dark frames are not usually taken. During the first Apogee observations it is verified that Apogee is on focus, otherwise the TO is asked to adjust the relative focus between MIRSI and Apogee.

During the observations   When observing a faint science target, it is usually first observed through the 11.6 µm filter which, among MIRSI's filters, is most sensitive to asteroid thermal emission. From the asteroid brightness in this filter it is estimated how long observations in other filters might take and whether challenging filters, such as the Q-band 18.4 µm filter, are tried at all.

During longer observations of a single target, we typically monitor its thermal

lightcurve in the 11.6 µm filter and intersperse observations in other MIRSI filters and Apogee V-band observations. It is particularly convenient to perform a quick Apogee observation while MIRSI is busy changing filters, which may take up to a minute.[5] For asteroid targets sufficiently bright to be observed with MIRSI, required Apogee integration times with the V filter are of the order of tens of seconds at most, while instrument changeover between Apogee and MIRSI is done within seconds.

During observations, all observation parameters are logged using the log sheets contained at the end of the MIRSI observer guide.[6] Most importantly, the observing time, duration, target name, filter, and airmass are logged in the designated columns. The "comments" column is used, among other things, for logging manual telescope offsets and changes to focus settings.

4.4 Data reduction

The measured asteroid flux is proportional to the detector response per integration time, the proportionality constant is determined from observations of calibration standard stars. The detector response to exposures is determined through synthetic aperture photometry after instrument-specific image-cleaning procedures.

Measured flux values must be corrected for the effect of atmospheric extinction ("airmass correction"). Corrections for the effect of finite filter breadth ("color correction") are discussed.

4.4.1 MIRSI

MIRSI data reduction is aided by a set of IDL routines developed by Eric Volquardsen, available on-line at `http://irtfweb.ifa.hawaii.edu/~elv` and described at `http://irtfweb.ifa.hawaii.edu/~elv/mirsi_steps.txt`. We use the routine `mirsi_coad` to remove instrument-specific artefacts and to coadd the observations taken at the four chop/nod beam positions with the appropriate signs. Note that cosmic ray hits are not a source of concern for MIRSI observations because their effect is dwarfed by the celestial background.

After coadding, MIRSI images display the source four times with two positive and two negative detections (see, e.g., Fig. 4.3 on p. 91). These four detections are copied pixel-wise into a single, "registered" detection after determining four

---

[5] This is a subjective estimate obtained during hectic observing nights.

[6] See `http://www.cfa.harvard.edu/mirsi/MIRSI_Obs_Guide.pdf`.

non-overlapping regions centered on each of the four detections and inverting the sign of the regions surrounding the negative detections. The edge length of these regions was chosen large enough to facilitate accurate background subtraction during synthetic aperture photometry, while guaranteeing that the region does not exceed the chip boundary. We typically use an edge length of 50 MIRSI pixels corresponding to 13.5″.

4.4.1.a Synthetic aperture photometry

Detector counts are determined by performing synthetic aperture photometry on the registered images. To this end, the pixel content of a synthetic aperture, i.e. a circular region surrounding the source centroid, is added up and corrected for the amount of background radiation contained inside the synthetic aperture. The background level is usually estimated from the pixel content of an annular region centered at the detection centroid. The background annulus should be far enough from the source to be uncontaminated with source flux but should be close enough to provide a good estimate of the local background level (which may be spatially variable). Accurate flux estimation from faint detections (low S/N) depends critically on appropriate background estimates. A practical criterion for the appropriateness of a background estimate is whether or not it leads to a stable photometric growthcurve (Howell, 1989)—see also the detailed discussion in Delbo' (2004, chapter 3).

Image registration and synthetic aperture photometry on MIRSI images can be automatized using the IDL routines by E. Volquardsen. We felt it was safer to perform these steps interactively, using the IDL-based registration and aperture-photometry tool by M. Delbo' (2004, sect. 3.6) which is a modified version of the ATV package by Aaron Barth (`http://www.astro.caltech.edu/~barth/atv/`). Image registration is done manually as described above. The synthetic aperture photometry routine automatically determines the centroid of the registered source. Care was taken to determine appropriate background values for each source by studying the photometric growthcurve. To avoid systematic uncertainties, the same aperture radius was chosen for all observations obtained during one observing run in a specific filter. To accommodate for possible temporal variations in the width of the point spread function, which may arise due to changes in seeing but also due to focus drifts, conservatively large aperture radii were chosen.

4.4.1.b Airmass correction

Fluxes determined from ground-based astronomical observations must be corrected for the effect of atmospheric extinction, which reduces the amount of flux received at the ground. Atmospheric extinction scales with the angular zenith distance of the observed target ζ, most conveniently expressed in terms of the airmass AM

$$\text{AM} := \frac{1}{\cos\zeta}. \tag{4.1}$$

To first order in airmass, the received fluxes f of a constant source observed at different airmasses are related by

$$-2.5\log\frac{f(\text{AM}_1)}{f(\text{AM}_2)} = E\,(\text{AM}_1 - \text{AM}_2) \tag{4.2}$$

with the extinction coefficient E in units of mag/airmass. Extinction coefficients for the Mauna Kea site depend greatly on the wavelength considered and may furthermore vary significantly from night to night (see, e.g., Krisciunas et al., 1987, and references therein); at infrared wavelengths, extinction coefficients depend chiefly on the atmospheric water content. A night during which extinction coefficients vary significantly is non-photometric by definition.

Practically, we determine extinction coefficients for each MIRSI filter and observing run by comparing the background-corrected detector response to observations of calibration standard stars at different wavelengths. While it is possible to relate observations of different calibration standard stars in this way, we tried to reobserve the same calibration standard whenever possible, in an attempt to minimize systematic uncertainties in the airmass correction (see sect. 4.3). Thus determined extinction coefficients were compared to the list compiled by Krisciunas et al. (1987) for the Mauna-Kea site, which serves as a useful cross-check.

Once the extinction coefficients are determined, all background-corrected detector counts are referred to the same airmass, where we typically use AM = 1. Larger values were occasionally chosen for observations which were obtained at large airmass.

4.4.1.c Flux calibration

After correction for background and airmass, detector counts C are proportional to the measured source flux f and the total on-source integration time t. Denoting quantities referring to the asteroid target with subscript a and quantities referring

to the calibration star with subscript s:

$$f_a = \frac{C_a}{t_a} f_s \frac{t_s}{C_s}. \tag{4.3}$$

Flux values for calibration stars were taken from Cohen et al. (1996, 1999).

4.4.1.d Color correction

As can be seen in table 4.1 on p. 87, MIRSI together with the filters used by us is a broad-band photometer, hence it would be expected that fluxes must be color corrected taking account of the target spectrum and the total spectral response of the combined telescope–filter–detector system (see sect. 5.2.4.g for a general discussion).

Determination of color-correction factors is here hampered by the lack of published filter transmission curves. Assuming a rectangular transmission curve centered at the central wavelength and with the spectral breadths given in table 4.1, Delbo' (2004, appendix B) determined color-correction factors for all MIRSI filters used by us and a number of black-body temperatures; the accuracy of his results is hard to estimate lacking information on the filter profile. For black-body temperatures between 200 and 400 K, which are appropriate for NEAs and MBAs, the thus determined approximate color-correction factors do not exceed a few percent, much below the remaining systematic and statistical uncertainties. Color corrections were therefore not applied to MIRSI fluxes.

4.4.2 Apogee

Like for MIRSI, the IRTF provides a set of IDL routines for the reduction of Apogee data developed by Eric Volquardsen (see `http://irtfweb.ifa.hawaii.edu/~elv` and `http://irtfweb.ifa.hawaii.edu/~elv/apogee_steps.txt`). The automatized data reduction steps include correction for bias and dark current, detection and removal of cosmic ray hits, synthetic aperture photometry, and airmass correction. We have carefully checked all pipeline elements (e.g. against our independent synthetic aperture photometry routine) and found them to work reliably for our high-signal-to-noise Apogee data. Only the detection and removal of cosmic ray hits requires visual inspection on a case-by-case basis to avoid flagging and "cleaning" parts of the source. The final product of the Apogee data reduction pipeline is an ASCII file containing instrumental magnitudes for all ob-

servations. Source magnitudes are determined by adding a constant magnitude offset determined from the instrumental magnitudes of the calibration standards (with V magnitudes listed in Landolt, 1973, 1992). By default, Volquardsen's IDL routines determine magnitudes of the brightest source in the field. Occasionally, Apogee's field of view contained field stars which were brighter (in the V band) than the asteroid target. In resulting image frames, the field star was masked semi-automatically prior to the proper data reduction, for which purpose we have developed an IDL routine.